Thermodynamic and Structural Stability of Cytochrome *c* Oxidase from *Paracoccus denitrificans*†

Tuomas Haltia,‡ Nora Semo,‡ José L. R. Arrondo,§ Felix M. Goñi,§ and Ernesto Freire*,‡

Departments of Biology and Biophysics and Biocalorimetry Center, The Johns Hopkins University, Baltimore, Maryland 21218, and Departamento de Bioquímica, Universidad del País Vasco, Aptdo. 644, E-48080, Bilbao, Spain

Received March 17, 1994; Revised Manuscript Received May 10, 1994®

ABSTRACT: The structural stability of the integral membrane protein cytochrome *c* oxidase from *Paracoccus denitrificans* has been measured by high-sensitivity differential scanning calorimetry and Fourier transform infrared spectroscopy. Contrary to the mammalian enzyme or the yeast enzyme, which are composed of 13 subunits, the bacterial enzyme has only three or four subunits, thus providing a unique opportunity to examine the magnitude of the forces that stabilize this enzyme and to establish accurate structural assignments of events observed calorimetrically. In this paper, experiments have been performed with the wild-type enzyme and with a mutant enzyme lacking subunit III. Our results show that subunits I and II form a highly cooperative complex which denatures as a single cooperative unit at 67 °C, while subunit III is less stable and denatures 20 °C earlier. Reduction of the enzyme causes a large increase in the stability of subunits I and II but has absolutely no effect on subunit III. Despite the lack of a strong interaction between subunit III and the catalytic subunits, the absence of subunit III leads to a turnover-induced loss of electron-transfer activity. The magnitude of the energetic parameters and the infrared spectroscopic experiments indicate that the enzyme does not completely unfold upon thermal denaturation and that significant degrees of structure are preserved. The amount of native α-helix structure, which is 45% in the native state, decreases only to 30% after thermal denaturation. Presumably, the residual helical structure existing after thermal denaturation belongs to the intramembranous portions of the protein. The calorimetric behavior of subunit III does not fully conform to that expected for a highly α-helical membrane protein. The picture that emerges from these experiments is that, in the temperature-denatured form of the enzyme, most of the extramembranous structural elements are denatured while most of the intramembranous secondary structure is maintained even though native tertiary interactions appear to be disrupted.

Integral membrane proteins are characterized by the presence of two distinct regions: (1) an intramembranous region embedded in the interior of the lipid bilayer and (2) one or more extramembranous regions that protrude to either side of the bilayer into the aqueous environment surrounding the membrane. The relative amount of protein mass located in the interior of the membrane varies significantly among proteins and can be less than 10%, as in the case of prostaglandin H synthase (Picot et al., 1994), or as high as 70–80%, as in the case of bacteriorhodopsin (Henderson et al., 1990). The energetics of stabilization of membrane proteins is expected to include contributions from these two regions in different proportions. The extramembranous regions are most likely stabilized by forces similar to those described for water-soluble proteins (Privalov & Gill, 1988; Murphy & Freire, 1992). The intramembranous regions, on the other hand, are believed to be extremely stable mainly because of the considerable strength of hydrogen bonds within the bilayer milieu [see Engelman et al. (1986), Popot and Engelman (1990), Cramer et al. (1992), and Yeates (1993) for reviews]. For water-soluble proteins, the relative contribution of hydrogen bonds to the stability of the protein is diminished by the fact that, upon protein unfolding, hydrogen bonds can be reformed with the solvent. This situation does not exist within the bilayer, accounting for the high stability of transmembrane α-helices and of the transmembrane β-barrel of porins (Cowan, 1993; Schulz, 1993). As a consequence of these energetic differences, the relative magnitude of the forces that stabilize the folded state of membrane proteins are expected to be distinct from those found in soluble proteins.

Heme–copper cytochrome oxidases are respiratory enzymes which function as the terminal oxidases of the mitochondrial and many bacterial respiratory chains [for reviews, see Babcock and Wikström (1992), Hosler et al. (1993), Malmström (1993), and Saraste (1990)]. Cytochrome *c* oxidase from *Paracoccus denitrificans* is a membrane protein with three subunits, each of which has characteristic properties: subunit I (558 amino acid residues, M_r = 62 500) has 12 hydrophobic segments which are believed to represent transmembrane α-helices (Raitio et al., 1990). It binds two hemes A and one copper ion (Cu_B). One of the hemes is hexa-coordinate and low spin (heme *a*), while the other (heme a_3) has a free coordination position and a high-spin electronic configuration. The high-spin heme together with Cu_B makes up the site for oxygen binding and reduction. Subunit II (252 residues, M_r = 27 999) has only two putative transmembrane spans with its major part being on the periplasmic side of the bacterial cell membrane (Raitio et al., 1987; Steinrücke et al., 1987). It is the latter soluble domain that contains the cytochrome *c* binding and electron entry sites of the enzyme (Capaldi et

† Supported by Grants GM37911 and RR04328 from the National Institutes of Health. T.H. has been partially supported by the Academy of Finland, the Finnish Cultural Fund, and the Magnus Ehrnrooth Foundation. J.L.R.A. and F.M.G. were supported by Grant No. 161/92 from the Universidad del País Vasco and Grant No. PB91-0441 from DGICYT.

‡ The Johns Hopkins University. Phone: (410) 516-7743. Fax: (410) 516-6469.

§ Universidad del País Vasco.

® Abstract published in *Advance ACS Abstracts,* July 15, 1994.

0006-2960/94/0433-9731$04.50/0

al., 1983; Lappalainen et al., 1993). Specifically, the electrons from cytochrome *c* are donated to a copper center known as Cu_A in the peripheral domain of subunit II (Hill, 1991). Recent studies suggest that the Cu_A center contains two copper atoms in a mixed-valence [Cu(II)–Cu(I)] configuration (Kroneck et al., 1988; Antholine et al., 1992; Kelly et al., 1993; Lappalainen et al., 1993). The sequence of subunit III (273 residues, M_r = 30 671) displays seven hydrophobic stretches that could span the membrane (Raitio et al., 1987). This subunit is very hydrophobic and does not contain any prosthetic groups. Some prokaryotic cytochrome *c* oxidases appear to contain a fourth subunit as well (Sone et al., 1990, 1993). Evidence for a putative fourth subunit in the *Paracoccus* oxidase is given in this paper.

The function of subunit III remains unknown (Brunori et al., 1987; Haltia et al., 1991), although a gene deletion study showed that it is important for the physiologically functional oxidase (Haltia et al., 1989). Deletion of the gene for subunit III resulted in a heterogeneous and partially inactive oxidase population. However, it is important to note that active cytochrome *c* oxidase molecules are present in the deletion mutant. As the phenotype of the mutant could be caused by assembled but unstable cytochrome oxidase, we decided to directly and quantitatively measure the stability of the active mutant enzyme.

Previously, we have investigated the structural stability of the mammalian and yeast cytochrome *c* oxidases (Rigell et al., 1985; Rigell & Freire, 1987; Morin et al., 1990). In both cases, it was found that subunit III is less stable and apparently does not interact strongly with the rest of the enzyme. Due to the complexity of the denaturation transition of a system containing 13 subunits, a detailed analysis of specific interactions between the main subunits could not be undertaken. The relative simplicity of the *Paracoccus* enzyme offers a unique opportunity to assess these intersubunit interactions.

In this paper, we have used high-sensitivity differential scanning calorimetry (DSC) and Fourier transform infrared (FTIR) spectroscopy to characterize the structural and thermodynamic stability of the dodecyl maltoside solubilized oxidase purified either from wild-type *Paracoccus* or from a mutant lacking the gene for subunit III. The experiments indicate that subunits I and II of the oxidase interact strongly in a redox-state-dependent manner, making up one structural entity, while subunit III constitutes another, structurally independent domain. The subunit III-less mutant enzyme is remarkably stable, behaving in DSC similarly to the complex of subunits I and II of the wild-type enzyme. Even though subunit III interacts only weakly with the rest of the complex, the absence of subunit III leads to a turnover-induced loss of activity, probably via an effect on the oxygen reduction site. These experiments have permitted identification of the structural components that undergo thermal denaturation and a quantitative dissection of the various energetic contributions to the stability of the enzyme.

MATERIALS AND METHODS

Materials. Dodecyl maltoside was obtained from Anatrace. Triton X-100 (reduced), cytochrome *c* (type VI), catalase (C-40) from bovine liver, glucose oxidase (G-7016) from *Aspergillus niger*, and Mn-containing superoxide dismutase (S-5639) from *Escherichia coli* were purchased from Sigma. Hydrogen peroxide was from Baker. Chromatographic media were obtained from Pharmacia.

Enzyme Purification. Unless otherwise stated, all steps were carried out at 4 °C. *Paracoccus denitrificans* strains 1657, 1222, and TN-57 were grown as described by Ludwig (1986). Membranes were prepared from 200–300 g of wet cells by using a French press. Cytochrome oxidase was purified as described by Haltia (1992a) with the following modifications: After the DEAE-Sepharose CL-6B step, the oxidase-containing fractions were chromatographed on an XK 26/10 column (Pharmacia) packed with Q-Sepharose high-performance resin. During this step, no EDTA was included in the buffers. Oxidase fractions from the Q-Sepharose column were concentrated by ultrafiltration and applied (following the suggestion of A. Warne, EMBL) to a chelating Sepharose fast flow column (Pharmacia XK 16/10), loaded with Cu(II) and equilibrated with 20 mM Tris-HCl, 0.5 M NaCl, and 0.03% dodecyl maltoside, pH 8.2. The chelating Sepharose column was developed using imidazole in the equilibration buffer. The column was first washed by increasing the imidazole concentration to 7.5 mM in 250 mL at 1.5 mL/min, after which the oxidase was eluted by elevating the imidazole concentration to 50 mM in 100 mL at 1 mL/min. Finally, oxidase fractions were concentrated and washed several times by dilution with 20 mM Tris-HCl and 0.03% dodecyl maltoside, pH 8.2, by using an ultrafiltration cell. The enzyme was frozen in aliquots in liquid nitrogen and was stored at −70 °C. When the oxidase was purified from the deletion strain TN-57 lacking the gene for subunit III (Haltia et al., 1989), only the autooxidizable fraction was collected in the chromatographic steps; this fraction behaves similarly to the wild-type enzyme in the above purification steps, whereas the reduced (inactive) fraction elutes at a lower salt concentration. The yield of the mutant oxidase was 15–20% of the total heme *a* present in the membrane fraction.

Subunit III depleted enzyme was prepared by incubating 10–20 μM wild-type oxidase with 3–4% Triton X-100 for 1 h on ice. The enzyme was then run twice through a Q-Sepharose XK 16/10 column equilibrated with 20 mM Tris-HCl, 0.5 mM EDTA, and 0.1% (w/v) Triton X-100, pH 8.2. Two-subunit oxidase elutes below 350 mM NaCl. In order to remove Triton, an excess of dodecyl maltoside was added to the pooled two-subunit oxidase fractions and the oxidase was rechromatographed on a Q-Sepharose column in the presesence of 0.03% dodecyl maltoside.

Protein Chemistry. Sodium dodecyl sulfate–polyacrylamide gel electrophoresis (SDS-PAGE) was carried out as described by Laemmli (1970) using 16% acrylamide concentration and 6 M urea in the gel. Samples were denatured at room temperature. A Coomassie Blue stained gel is shown in Figure 1A. The differential detergent solubility experiment was performed as described by Rigell and Freire (1987). For N-terminal sequencing of the putative fourth subunit, which migrates similarly to the yeast cytochrome *c* oxidase subunit VII (M_r = 6603; Power et al., 1986) (see Figure 1A), 600 pmol of the oxidase was electrotransferred onto a poly(vinylidene difluoride) (PVDF; Bio-Rad) membrane using the SDS–PAGE buffer containing 20% (v/v) methanol. The PVDF membrane was stained with Coomassie Blue and destained as advised by Bio-Rad. The protein band was cut out and applied to an Applied Biosystems 470A protein sequenator. A 31-residue long hydrophilic sequence was obtained (see Table 1). To determine whether the fourth polypeptide is a stoichiometric component of the oxidase complex, about 600 pmol of the native bacterial oxidase in 20 mM K-Hepes and 0.03% dodecyl maltoside, pH 7.4, was applied to the sequenator. Since subunits I and II have blocked N-termini (Steffens et al., 1983), each sequencing cycle should yield only two amino acid derivatives, one from subunit III

Table 1: Stoichiometry of Subunit III (COIII) and the Putative Fourth Subunit (COIV)[a]

COIII			COIV		
cycle no.	residue	yield (pmol)	cycle no.	residue	yield (pmol)
1	A	305.8	1	A	305.8
2	H	105.2	2	S	141.5
3	V	261.8	3	H	133.8
4	K	211.5	4	H	153.0
5	N	198.1	5	E	199.4
6	H	120.2	6	I	209.8
7	D	151.7	7	T	150.8
8	Y	212.0	8	D	190.6
9	Q	206.8	9	H	164.9
10	I	190.0	10	K	174.6

[a] The N-terminal sequence of the putative fourth subunit is ASHHE ITDHK HGEMD IRHQQ ATFAG FIKGA T. The yield in cycle no. 1 equals the total uncorrected yield divided by 2. The yield of each PTH amino acid identified in cycle N was background corrected by subtracting the signal of the same PTH amino acid in cycle $N - 1$. The yields of PTH–histidines were not corrected. The recoveries of S, T, and H are generally lower.

and the other from the putative subunit IV, which was found to be the case. Since both sequences are known, comparison of the yields gives an estimate of the relative amounts of the two subunits.

Cytochrome c Oxidase Activity. Oxidase activity was measured polarographically at room temperature using a Clark-type oxygen electrode equipped with an 8-mL cell. The buffer used was 50 mM K-Hepes, 50 mM KCl, 0.5 mM EDTA, and 0.03% dodecyl maltoside, pH 7.2, supplemented with 5 mM ascorbate, 25 μM cytochrome *c*, and 0.5 mM tetramethyl-*p*-phenylenediamine (TMPD). Typical catalase and hydrogen peroxide additions were 300 μg and 30 μL of 0.3% H_2O_2 (see Figure 2). In some experiments, 1 mg/mL asolectin (Associated Concentrates) was present in the buffer. Steady-state reduction levels of heme *a* were monitored at 605 nm using a Perkin-Elmer 4B spectrophotometer. The oxidase was diluted to 1 μM with 50 mM K-Hepes, 1 mM EDTA, and 0.05% dodecyl maltoside, pH 7.2. Ten millimolar ascorbate and 2 μM horse heart cytochrome *c* were added, resulting in a steady state that lasted about 6 min. Cytochrome oxidase concentrations were determined using a millimolar absorptivity of 23.4 cm^{-1} at 605 nm minus 630 nm (reduced minus oxidized) (Ludwig & Schatz, 1980).

Microcalorimetry. For DSC, the oxidase was dialyzed against 1000 mL of 10 mM KP_i, 300 mM NaCl, 0.03% dodecyl maltoside, and 0.75 mM EDTA, pH 8.2, for 6–8 h and then overnight against 1000 mL of 10 mM KPi, 300 mM NaCl, 0.03% dodecyl maltoside, and 0.3% glucose, pH 8.2. Experiments were performed with the enzyme in the oxidized and the reduced state. For the calorimetric experiments, 40 μg/mL glucose oxidase, 4 μg/mL catalase, and 1 μg/mL superoxide dismutase were added to both the sample and the reference cell of the calorimeter prior to scanning. This procedure was utilized to deplete the solutions of oxygen. The enzyme was reduced by adding 2 mM dithionite from a 100 mM stock solution made in 100 mM KP_i, pH 8.2. Typically, the presence of reductant brought about some baseline instability at high temperatures which, however, did not preclude detection of the protein transitions. DSC scans were performed with sample concentrations ranging between 2 and 4 mg/mL at a scanning rate of 1 °C/min using a DASM-4M instrument interfaced to an IBM PC. The analysis of the data was performed with software developed in this laboratory as described before (Freire et al., 1990; Morin et al., 1990).

Fourier Transform Infrared Spectroscopy. Samples for FTIR spectroscopy were made up in D_2O using the same buffers as in DSC but without the glucose oxidase system. Spectra acquisition and resolution enhancement were performed as described previously (Prado et al., 1990; Castresana et al., 1992). Protein concentration was ~25–30 mg/mL (~0.2 mM). Quantitative information on protein structure was obtained through decomposition of the original amide I band into its constituents. The curve-fitting method used has been described earlier (Arrondo et al., 1989; Castresana et al., 1988; Fernandez-Ballester et al., 1994). For thermal treatment, samples in D_2O buffer were heated in steps of ~2.5 °C in the interval 20–80 °C. After every heating step the sample was left to stabilize for 5 min, and the corresponding spectrum was recorded and treated as described above. The entire set of operations between two consecutive heating steps took 30 min.

RESULTS AND DISCUSSION

Enzyme Preparations and Oxidase Activity. Figure 1A shows a SDS–PAGE analysis of the wild-type cytochrome *c* oxidase from *Paracoccus denitrificans* ($pCOX_{wt}$) and a mutant enzyme lacking subunit III ($pCOX_{III-}$). As expected, the autooxidizable fraction of the mutant enzyme (lane 2) is composed of subunits I and II only. However, the wild-type oxidase (lane 1) contains, in addition to subunit III, a fourth polypeptide which migrates similarly to the yeast oxidase subunit VII (lane 3) (M_r = 6603). This peptide copurifies with the oxidase in a reproducible manner and has been observed before (Haltia, 1992b; Steverding et al., 1993). Additional experiments were performed in order to characterize the origin of this peptide. The 31 amino acid residue long N-terminal sequence of the peptide, shown in Table 1, appears not to be homologous to any known protein. Application of the whole oxidase complex to a sequenator yields two equally intense sequences, one representing subunit III and the other, the putative fourth subunit (see Table 1). The small hydrophilic peptide appears to be a stoichiometric component of the complex, and it may bind to the oxidase complex via subunit III, as it is not observed in preparations lacking subunit III or in the mutant $pCOX_{III-}$ [cf. Steverding et al. (1993)].

Figure 2 shows polarographic activity assays of the wild-type oxidase and two types of preparations lacking subunit III. Two points should be noted: First, both $pCOX_{III-}$ and the subunit III depleted preparation of $pCOX_{wt}$ exhibit substantial activity, albeit less than a third of that of the intact wild-type preparation. Second, both types of preparations lacking subunit III become inactivated during steady-state catalysis, and their activity cannot be restored by introducing additional oxygen into the measuring cell. These experiments suggest that the reason for the loss of activity is not a decreased affinity toward oxygen and that turnover is essential for the inactivation. In contrast, the wild-type enzyme turns over without inhibition for long periods of time until all reductant is consumed if enough O_2 is provided. Conceivably, the absence of subunit III causes a subtle structural perturbation of the oxygen reduction site. This conclusion is supported by the observation that the steady-state reduction level of heme *a* is higher in $pCOX_{III-}$ than in $pCOX_{wt}$ even under low-turnover conditions (data not shown). Also, one should note that the slightly perturbed active site might be the primary reason for the impaired oxidase function in the mutant.

Differential Scanning Calorimetry of the Oxidized Enzyme. Figure 3 (panel A) shows the temperature dependence of the

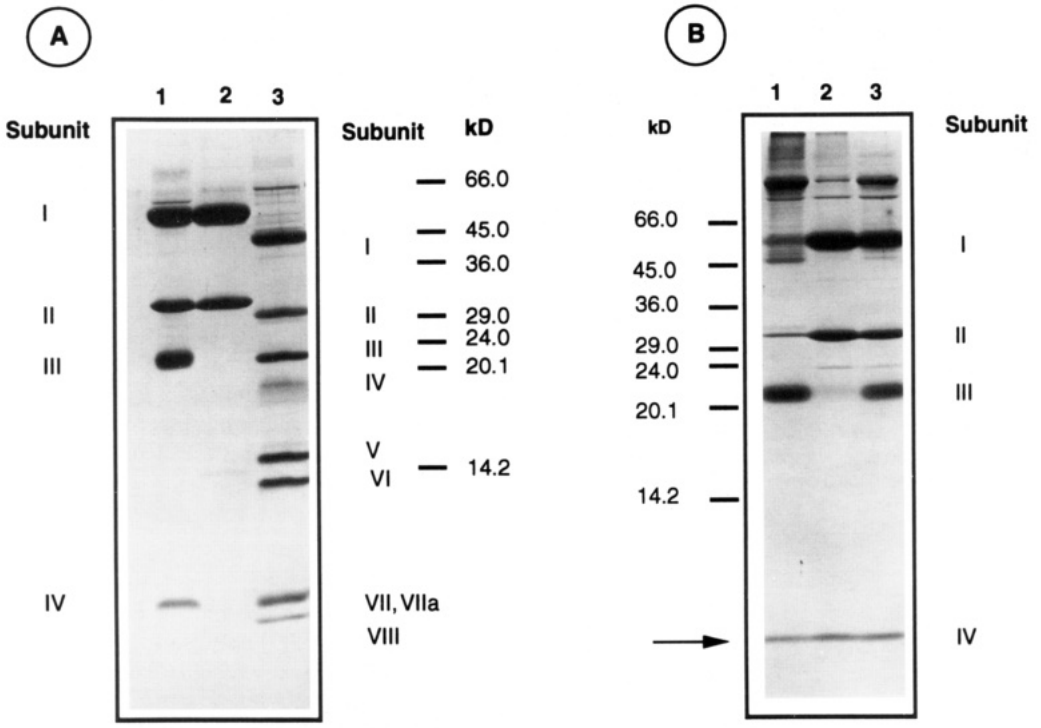

FIGURE 1: (A) SDS–polyacrylamide gel electrophoresis of the *Paracoccus* oxidase preparations used in the DSC and activity measurents. Lane 1, wild-type oxidase; lane 2, oxidase from the mutant lacking the gene of subunit III; lane 3, a yeast oxidase preparation purified using cholate, included to serve as an additional molecular mass marker. The subunits of the yeast oxidase and the molecular mass scale are indicated on the right; the subunits of the bacterial oxidase are assigned on the left. IV denotes the putative fourth subunit, which migrates as the yeast subunit VII (M_r = 6603) and is close to stoichiometric with subunit III. (B) SDS–polyacrylamide gel electrophoresis of an oxidase sample heated to 58 °C and centrifuged. The gel shows that subunit III denatures and precipitates quantitatively below 58 °C, whereas subunits I and II remain soluble and folded. Lane 1, pellet after heating; lane 2, supernatant after heating; lane 3, not heated. In the purification of the preparation used in this experiment the chelating Sepharose step was omitted, and the preparation therefore contains some high molecular weight impurities. A molecular mass scale and the subunit assignments are on the left and right, respectively. The putative fourth subunit (arrow) appears not to precipitate completely in the experiments, probably owing to its hydrophilic nature. However, some of it appears in the pellet with subunit III, suggesting that it is mainly associated with this subunit.

excess heat capacity function of the wild-type cytochrome *c* oxidase from *Paracoccus denitrificans* ($pCOX_{wt}$) in the oxidized state. The calorimetric scan is characterized by two well-separated peaks centered at 48 and 68 °C, respectively. The total enthalpy change for the thermal denaturation of the enzyme is 370 kcal/mol. Unlike other membrane proteins, the heat denaturation of $pCOX_{wt}$ yields a clean calorimetric scan in which a ΔC_p between the denatured and the native state is clearly observed. This ΔC_p is close to 12 kcal/(mol K). As is the case with the beef and yeast oxidases, the thermal denaturation of $pCOX_{wt}$ is a kinetically controlled irreversible process and cannot be analyzed with the equations of equilibrium thermodynamics (Rigell et al., 1985; Rigell & Freire, 1987; Morin et al., 1990). The deconvolution of the heat capacity curves was therefore performed in terms of a multistate irreversible model as described previously for the yeast oxidase (Morin et al., 1990). According to this model, the transition is represented as a sum of independent irreversible processes of the form ($N_i \rightarrow D_i$) in which each transition is characterized by an enthalpy change (ΔH), a heat capacity change (ΔC_p), and an activation energy ($\Delta H^{\dagger}$); the observed transition temperature is a function of the scanning rate at which the experiment is performed (Freire et al., 1990; Morin et al., 1990). The magnitude of the activation enthalpy (Table 2) is similar to that found for the yeast enzyme (Morin et al., 1990). The activation enthalpy determines the temperature dependence of the rate of denaturation of the protein.

Analysis of the data indicates that the thermal denaturation of $pCOX_{wt}$ is well represented by the sum of two transitions as illustrated in Figure 3A. In this figure the solid line is the theoretical curve calculated with the parameters in Table 2. These results indicate that $pCOX_{wt}$ is composed of two independent cooperative folding units, each of which can be closely approximated by a two-state transition mechanism. Figure 3B shows the calorimetric scan obtained for a sample of the oxidized mutant enzyme lacking subunit III ($pCOX_{III^-}$). It is clear from this scan that the low-temperature peak is missing, suggesting that this endotherm corresponds to the thermal denaturation of subunit III. The transition peak is centered at the same temperature as the high-temperature peak in the wild-type enzyme, even though in the mutant enzyme it appears broader and less cooperative. The small shoulder on the high-temperature side of the mutant thermogram occurs at the same temperature as the transition of the reduced mutant enzyme (see Figure 4), suggesting that it is caused by a small amount of reduced enzyme that copurifies with the oxidized form. The heat capacity change for $pCOX_{III^-}$ is 7.1 kcal/(K mol), and the total enthalpy change is 250 kcal/mol, in excellent agreement with the values obtained from the deconvolution of the wild-type enzyme thermogram. While the overall parameters are similar, it is clear that the curve in Figure 3B exhibits a broader component in addition to the sharp peak centered at 67 °C, suggesting that the absence of subunit III influences the complex formation of subunits I and II. In the wild-type enzyme, the high-temperature peak corresponding to subunits I and II conforms closely to a two-state mechanism indicating a high degree of cooperative interactions between the two subunits. These interactions appear to be diminished in the mutant enzyme. Also, we have noticed that, in enzyme preparations

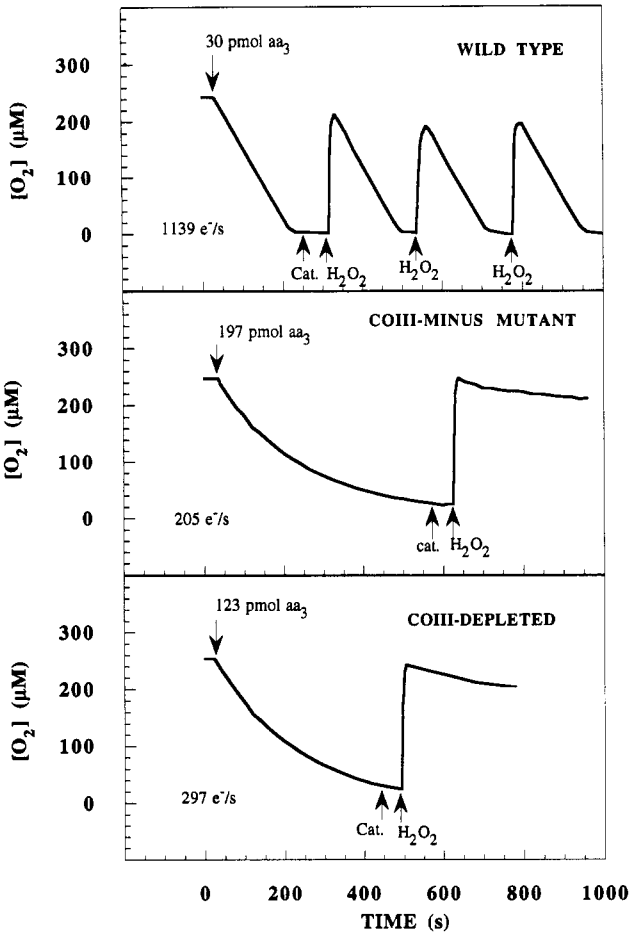

FIGURE 2: Polarographic activity measurements of $pCOX_{wt}$, $pCOX_{I-II}$-, and subunit III-less wild-type oxidases using a Clark-type oxygen electrode at room temperature. The initial molecular activity of each preparation, calculated from the slope of the traces, is shown. Note the inactivation of both subunit III-less preparations. aa_3 = cytochrome *c* oxidase; Cat. = catalase; COIII = subunit III.

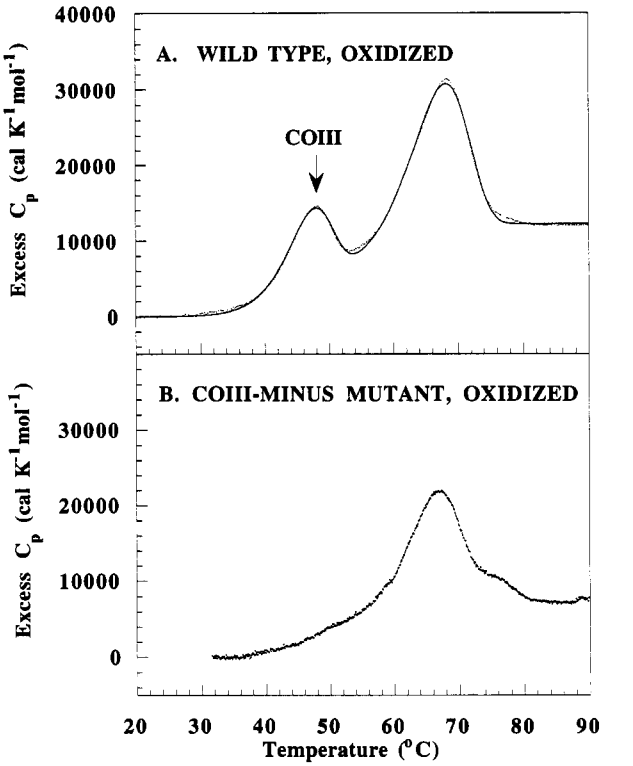

FIGURE 3: DSC scans of the oxidized $pCOX_{wt}$ (panel A) and $pCOX_{III}$- (panel B) enzymes. COIII = subunit III. The heat capacity function was analyzed in terms of a multistate kinetic model as described in the text. The solid line is the theoretical curve calculated with the parameters in Table 2.

Table 2: Thermodynamic Parameters for the Thermal Denaturation of Oxidized Cytochrome *c* Oxidase from *Paracoccus denitrificans*

transition	T_m (°C)	ΔH (kcal/mol)	ΔC_p [kcal/(K mol)]	$\Delta H^\dagger$ (kcal/mol)	subunit assignment
1	46.7 ± 0.2	101 ± 10	5.2 ± 0.5	53 ● 5	III
2	67.0 ± 0.2	272 ± 20	7.0 ± 0.5	47 ● 5	I and II

obtained by lysing the cells with osmotic shock, the cooperative interactions between subunits I and II might be somewhat weaker, giving rise to two components in the high-temperature peak.

The assignment of the low-temperature transition to subunit III, on the basis of the comparison of the calorimetric scans of the wild-type and mutant enzymes, was confirmed by performing differential detergent solubility experiments as described before (Rigell et al., 1985; Rigell & Freire, 1987; Morin et al., 1990). This technique is based on the observation that native subunits of membrane proteins can be solubilized by much lower detergent concentrations than denatured subunits. So, under conditions in which some subunits are denatured and other subunits are in the native state, it is possible to separate them by centrifugation in the presence of a concentration of detergent capable of solubilizing only the native subunits. As shown in Figure 1B, after the wild-type enzyme is heated to 58 °C, a temperature intermediate between the low- and high-temperature peaks, subunit III is no longer solubilized by the detergent and is only present in the pellet. This experiment confirms the assignment of the low-temperature peak to subunit III. In this respect, the bacterial oxidase is similar to the beef and yeast enzymes in which subunit III is also the one with the lowest transition temperature.

Effects of State of Oxidation on Thermal Stability. Figure 4 shows the heat capacity function of $pCOX_{wt}$ in the reduced state. In this case, the low-temperature peak is centered at 46.7 °C and the high-temperature peak is centered at 76 °C. This result indicates that the state of oxidation does not directly or indirectly affect the stability of subunit III, since the low-temperature peak remains at the same location even though the transition temperature of the main peak is increased by nearly 10 °C. In both reduced and oxidized states the main peak is highly cooperative and closely conforms to two-state behavior under the experimental conditions presented here. In the reduced state the transition becomes sharper, a consequence primarily of the larger enthalpy expected at higher temperatures due to the existence of a ΔC_p. Since subunit I carries the two heme groups of the molecule, it seems plausible that this subunit is the one primarily affected by the state of oxidation and that the resulting changes are propagated to subunit II. More specifically, the sequence of events could be initiated by a ruffled-to-planar change in the geometry of the heme *a* porphyrin ring after reduction (Heibel et al., 1993). The extent of the protein conformational change appears to be small, however: compared to the FTIR spectrum of the oxidized sample, the spectrum of the reduced oxidase, measured at 25 °C, exhibits only minor changes. These changes involve mainly the bands at 1644 and 1630 cm^{-1} (data not shown). An exchange of these two components suggests a decrease in the quantity of β-sheets concomitant with an increase in loops or nonstructured segments. This exchange is reverted upon reoxidation, and it also involves small changes in β-turns. A similar effect has been observed in the nicotinic acetylcholine receptor upon agonist binding

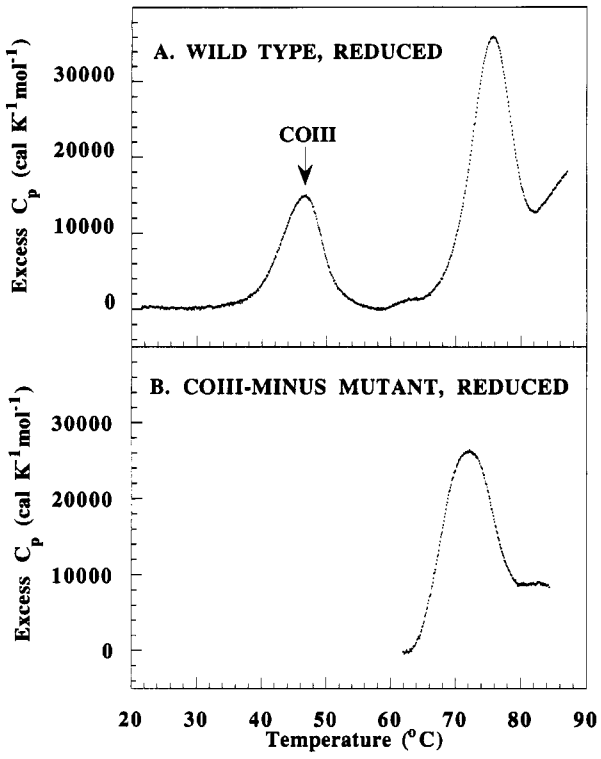

FIGURE 4: DSC scans of the reduced $pCOX_{wt}$ (panel A) and $pCOX_{III-}$ (panel B) enzymes. COIII = subunit III. As discussed in the text, the presence of a reducing agent affects the baseline stability of the instrument. Nevertheless, the transition peaks associated with the enzyme could be detected.

(Castresana et al., 1992). Although these changes are not extensive, they may be important for function [see Haltia (1992a) and Thomas et al. (1993)]. Subtle redox-linked infrared spectral changes have also been detected in beef heart oxidase by derivative spectroscopy (Caughey et al., 1993).

The effect of reduction was qualitatively similar with $pCOX_{III-}$ (Figure 4). As with the oxidized mutant enzyme, the transition profile is broader when compared with that of the wild-type enzyme, suggesting a diminished intersubunit cooperativity. In this case, the T_m does not increase as much as with the wild-type enzyme. The latter observation indicates that the mutant has a less stable reduced state than the wild type, probably due to a lower midpoint potential. These differences with the wild-type enzyme are consistent with the idea proposed earlier (Haltia et al., 1989) that subunit III affects the assembly of the two other subunits.

The Magnitude of the Denaturation Energetics. Cytochrome *c* oxidase, like other integral membrane proteins, is composed of a region embedded within the lipid bilayer and a region located outside the bilayer and exposed to the aqueous medium. The recent electron crystallographic study by Frey and Murray (1994) suggests that there might in fact be three intramembrane domains in the eukaryotic oxidase, viz., two major domains called M1 and M2 plus a minor one called X. The latter appears rather separate from the other two, and within the context of the results presented here it is tempting to speculate that it comprises a part of subunit III. In the case of the beef oxidase molecule, it is thought that at least 50% of the total mass is located outside the membrane (Deatherage et al., 1982; Valpuesta et al., 1990; Frey & Murray, 1994). In particular, the active site is thought to be close to the outer surface of the membrane (Hosler et al., 1993). Thus, in the analysis of the denaturation energetics it is necessary to account for the extra- and intramembranous portions of the protein.

The extramembranous regions of membrane proteins are expected to exhibit unfolding energetics similar to that of water-soluble proteins; i.e., the disruption of secondary and tertiary structure interactions is accompanied by the hydration of the groups that become unfolded. The situation with the intramembranous regions of the membrane is very different. In this case, the interior of the lipid bilayer lacks hydrogen bond donor or acceptor groups that compete for intramolecular or intermolecular protein hydrogen bonds. As a result, secondary structure elements within the lipid bilayer exhibit extremely high stability (Engelman et al., 1986; Popot & Engelman, 1990; Zhang et al., 1992; Yeates, 1993). Engelman et al. (1986) have estimated that the free energy of stabilization of a 20-residue transmembrane helix inside the bilayer is on the order of 70 kcal/mol. For comparison, water-soluble proteins have maximal free energies of stabilization anywhere between 5 and 15 kcal/mol. A major component of this difference is expected to be of enthalpic origin. Since the disruption of hydrogen bonds is not accompanied by the reformation of those bonds with the solvent, the enthalpy change for the disruption of secondary and tertiary structure within the bilayer is expected to be much higher than in aqueous solution. In addition, hydrophobic groups that remain inside the bilayer upon denaturation do not become hydrated and do not contribute the negative enthalpy associated with the hydration of apolar groups (Murphy & Freire, 1992). In summary, complete unfolding within the bilayer with no exposure to water must be accompanied by a high enthalpy change.

As discussed above, the total enthalpy associated with the thermal denaturation of $pCOX_{wt}$ is 370 kcal/mol, or 2.92 cal/g when normalized on a weight basis. This value is significantly lower than the enthalpy change associated with the unfolding of water-soluble proteins. For water-soluble proteins, the average ΔH for the entire database at the experimental denaturation temperature of 67 °C is 7.8 ± 0.7 cal/g (Murphy et al., 1992). The corresponding enthalpy changes for the denaturation of the beef heart and yeast oxidases are about 2.7 and 2.4 cal/g, respectively (Rigell et al., 1985; Rigell & Freire, 1987; Morin et al., 1990). These results suggest that the thermal denaturation of cytochrome oxidase does not lead to the unfolding of the entire molecule.

The second important quantity to be considered is the heat capacity change associated with thermal denaturation, which amounts to 12 kcal/(K mol), or 0.096 cal/(K g), for $pCOX_{wt}$. For comparison, the average heat capacity change for the unfolding of water-soluble proteins is 0.13 ± 0.02 cal/(K g); for myoglobin, a protein with one of the most hydrophobic cores, ΔC_p is 0.15 cal/(K g), and for ribonuclease A, a protein with one of the least hydrophobic cores, ΔC_p is 0.10 cal/(K g). If we consider that $pCOX_{wt}$ contains a higher proportion of buried apolar residues than myoglobin, then the complete unfolding and exposure to water of $pCOX_{wt}$ must be accompanied by a ΔC_p of at least 0.15 cal/(K g). The experimental value of 0.096 cal/(K g) indicates that the thermal denaturation of $pCOX_{wt}$ is accompanied by the hydration of only a portion of the molecule. Additional experiments performed at different salt concentrations (not shown) suggest that the actual magnitude of ΔC_p might be ionic strength dependent.

Structural Analysis. The location of the transmembrane segments of subunits I, II, and III has been the subject of analysis by Chepuri and Gennis (1990) and Saraste (1990). On the basis of hydrophobicity plots and gene fusion experiments, these authors have identified the putative

Table 3: Locations of Transmembrane Segments in Subunits of Cytochrome c Oxidase from *Paracoccus denitrificans*[a]

subunit I segment	residues	subunit II segment	residues	subunit III segment	residues
I	31–53	I	64–85	I	14–35
II	87–112	II	106–128	II	49–67
III	131–151			III	89–114
IV	183–206			IV	141–164
V	219–246			V	174–201
VI	270–290			VI	204–232
VII	308–330			VII	246–272
VIII	339–364				
IX	373–396				
X	405–428				
XI	449–471				
XII	491–513				

[a] Subunit I, II, and III sequences are from Raitio et al. (1990), Steinrücke et al. (1987), and Raitio et al. (1987), respectively.

locations of the transmembrane helices in the three subunits. Subunit I, which is composed of 558 amino acids, contains 12 long hydrophobic segments involving approximately 264 amino acids. Subunit II, on the other hand, is composed of 252 amino acids and exhibits only two adjacent hydrophobic segments located near the N-terminus. It is believed that this subunit consists of two parts: a helix hairpin embedded in the membrane and a larger (151 amino acids) C-terminal domain that resides outside the membrane [cf. Lappalainen et al. (1993)]. Subunit III is composed of 273 amino acids and exhibits seven hydrophobic sequences with a total of 174 amino acids. The sequence and transmembrane helix assignments of Saraste (1990) are summarized in Table 3.

If it is assumed that all of the hydrophobic segments identified by the hydropathy analysis are transmembrane helices, the overall helical content of $pCOX_{wt}$ would be at least 45%, i.e., if there were no helices in the extramembranous portions of the molecule. Subunits I and III exhibit the highest proportion of residues within the membrane (47 and 64% respectively), while subunit II only buries 18% of its amino acids within the lipid bilayer.

The structural parameters above permit setting some limits to the magnitude of the thermodynamic parameters for the unfolding of the different regions of the molecule. First, if we assume that the putative extramembranous regions of the protein behave as regular water soluble proteins, the ΔC_p for unfolding is expected to range between 3.2 and 4.8 cal/(K mol) for subunit I, between 1.7 and 2.5 kcal/(K mol) for subunit II, and between 1.1 and 1.65 kcal/(K mol) for subunit III, using the range of experimental values for water-soluble proteins discussed above. The thermal denaturation of subunits I and II corresponds to the major peak in the thermogram and has a ΔC_p that amounts to 7.0 kcal/(K mol). This value falls within the range of 4.9–7.3 kcal/(K mol) expected for the extramembranous regions predicted for these subunits. On the other hand, the enthalpy change expected for the extramembranous regions of subunits I and II is on the order of 346–414 kcal/mol compared to the experimental value of 272 kcal/mol. For subunit III the experimental ΔC_p of 5.2 kcal/(K mol) is considerably larger than the value expected for the putative extramembranous regions only. In this case the expected enthalpy for the extramembranous regions at the experimental transition temperature of 47 °C ranges between 50 and 65 kcal/mol, which is significantly lower than the experimental value of 101 kcal/mol.

The heat capacity change provides a direct measure of the hydration of protein groups upon denaturation (Privalov & Gill, 1988; Murphy et al., 1992; Murphy & Freire, 1992; Spolar et al., 1992). The values obtained for subunits I and II are consistent with the unfolding and hydration of the putative extramembranous regions. The experimental enthalpy change, on the other hand, is about 100 kcal/mol smaller than that expected for the extramembranous regions. Again, assuming that the structural assignments are correct, this result would indicate that the extramembranous portion is not completely unfolded and that it retains some structure after denaturation.

In the case of subunit III, the experimental heat capacity and enthalpy changes are significantly larger than the ones expected for the putative extramembranous regions only. This suggests either that a significant portion of the intramembranous region of subunit III also becomes exposed to water and partially unfolds or that some of the hydrophobic segments that have been considered to be transmembrane helices actually form part of the extramembranous regions and become unfolded. It is noteworthy that several pieces of data in the literature show that subunit III is very asymmetrically situated in the membrane [see Wikström et al. (1981) for a review], being much more exposed to the outer than to the inner side of the membrane (Zhang et al., 1988), suggesting that its extramembranous portions are actually larger than those predicted by the hydropathy analysis. In addition, there are some data which appear not to be compatible with the current topological model of subunit III deduced from gene fusion experiments [cf. Casey et al. (1981), Chepuri and Gennis (1990), Degli Esposti et al. (1990), and Saraste (1990)]. Also, in guanidine hydrochloride denaturation experiments, subunit III does not behave as expected for an α-helical membrane protein (Hill et al., 1988).

Infrared Spectroscopic Analysis of Thermal Denaturation. The magnitude of the enthalpy and heat capacity changes suggests that only part of the molecule unfolds upon thermal denaturation. In particular, subunits I and II may not unfold completely. Judging by the experimental values, it appears that the extramembranous regions are the ones that undergo thermal denaturation, while the intramembranous regions remain folded at all temperatures. This hypothesis was tested by examining the structural changes that take place during thermal denaturation.

Figure 5 shows the effect of temperature on the amide I and amide II bands in the deconvolved infrared spectra of $pCOX_{wt}$ in a D_2O buffer. At high temperatures, the appearance of two bands around 1686 and 1620 cm^{-1} is usually indicative of protein aggregation (Muga et al., 1993) and is correlated with a loss of the residual amide II, indicating an increased accesibility of the protein core to deuterium exchange. This has been related to an "opening up" of the protein (Yang et al., 1987). It should be noted that the bands at 1515 and 1580 cm^{-1}, corresponding to amino acid side chains, do not change after thermal denaturation and that the amide I band is still structured. Two spectra of $pCOX_{wt}$ in D_2O, recorded respectively at 18 (bottom) and 77 °C (top), are shown in Figure 6, together with the result of band decomposition analysis. In the thermally treated sample the α-helix band at ca. 1658 cm^{-1} is somewhat broader than at room temperature, implying a less structured α-helix, i.e., a higher number of α-helical conformational variants. The temperature dependence of the position and percent area of the α-helix components is shown in more detail in Figure 7. Rather sharp transitions are observed for band position ($T_m \sim 59$ °C) and percent area ($T_m \sim 48$ °C). The difference in T_m suggests that two separate processes are observed: the unfolding of a fraction of the helical structure, leading to a decrease in the

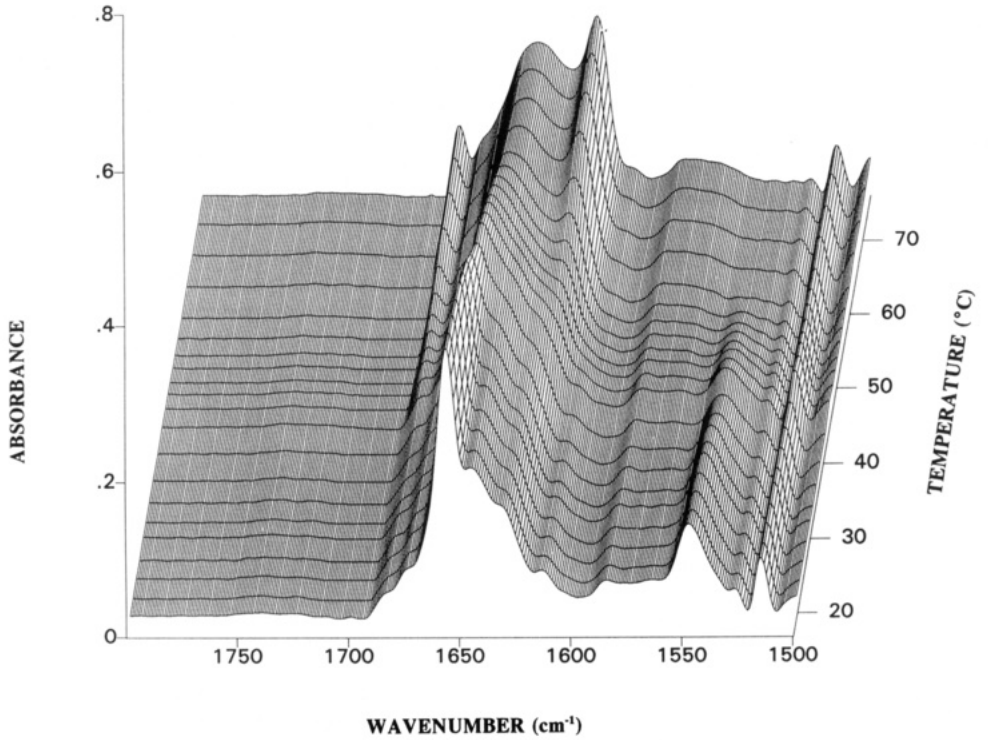

FIGURE 5: Infrared deconvolved spectra in a D_2O buffer of the oxidized $pCOX_{wt}$ as a function of temperature. The deconvolution parameters were a bandwidth of 18 cm^{-1} and an enhancement factor (K) of 2. Note the appearance of bands at 1686 and 1620 cm^{-1} when the temperature is elevated.

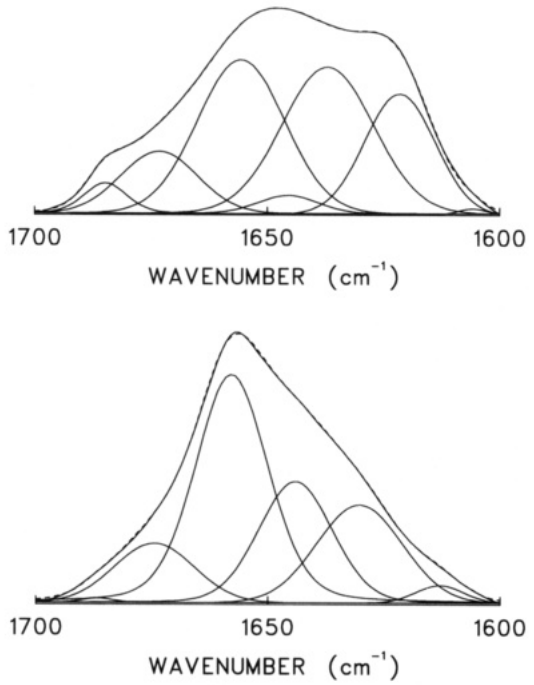

FIGURE 6: Band decomposition of the original amide I band at 18 (bottom) and 77 °C (top). The spectra were baseline corrected prior to the decomposition procedure. The ordinate axis is the same for both spectra. The band at 1658 cm^{-1} reflects the amount of α-helix.

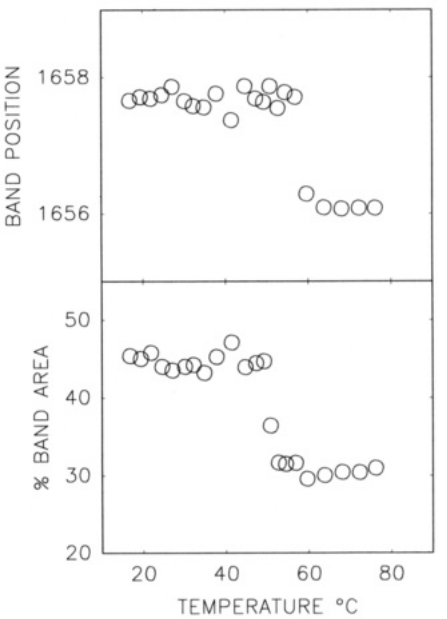

FIGURE 7: Plots of band position (top) and percentage band area (bottom) versus temperature of the amide I component around 1658 cm^{-1}. To obtain the percentage band area, the bands below 1615 cm^{-1}, corresponding to amino acid side chains, were not considered.

component at 1658 cm^{-1}; and at higher temperatures, a slight change in conformation of the remaining α-helices. The exact temperature location of these changes is somewhat lower than in the calorimetric scans due to the much slower rate of heating used in the FTIR experiments.

Decomposition of the spectra obtained at room temperature indicates that the native wild-type protein is about 45% α-helical (Figures 6 and 7). Unless the extramembranous portions of the oxidase molecule are completely devoid of helical structure, this value suggests that the prediction of the hydropathy analysis overestimates the number of transmembrane helices. The FTIR data clearly demonstrate the thermostability of the helical structures: two-thirds of the helices do not melt, and even at 77 °C the helical content is 30%. Interestingly, 30% helicity would correspond to about 14 "full-length" transmembrane helices. This value agrees quite well with the number of transmembrane helices estimated by electron microscopy of 2D crystals of the beef oxidase (Capaldi, 1990; Valpuesta et al., 1990), which is less than the number predicted by the hydropathy analysis. In the light of

the above discussion, the thermostable helices may represent mainly, if not exclusively, the transmembrane segments of the oxidase.

CONCLUSIONS

The results presented in this paper indicate that most helical domains of the catalytic subunits of cytochrome *c* oxidase do not undergo thermal unfolding and that these domains most likely correspond to transmembrane helices. Both the energetics of thermal denaturation and the FTIR analysis are consistent with the persistence of most of the helical structure after thermal denaturation. This behavior is also expected for other α-helical membrane proteins. Besides cytochrome *c* oxidase, high-sensitivity differential scanning calorimetry has been performed on bacteriorhodopsin (Brouillette et al., 1987, 1989). In this case the protein denaturation transition is centered at 100 °C and has a calorimetric enthalpy of approximately 100 kcal/mol (3.7 cal/g), which is also substantially smaller than that of a typical soluble protein at the same temperature. Reported ΔC_p values are also extremely small, indicating that thermal denaturation is not coupled to significant hydration of the polypeptide chain. Spectroscopic experiments on bacteriorhodopsin and on the band 3 protein (Brouillette et al., 1987; Shnyrov & Mateo, 1993; Oikawa et al., 1985) also support the idea that the intramembranous portions of membrane proteins do not become unfolded upon thermal denaturation. Solvent denaturation of beef heart cytochrome *c* oxidase (Hill et al., 1988) and yeast oxidase (unpublished results) is a biphasic process in which one part of the oxidase loses its secondary structure at low concentrations of the perturbant while another part of the enzyme retains a large fraction of its helicity even at the highest denaturant concentrations used. These results suggest that the extra- and intramembranous regions of membrane proteins have vastly different stabilities. In general, the stability of the intramembranous regions is extremely high, permitting unfolding or major conformational rearrangements of the extramembranous regions without significant repercussions on the transmembrane domains. These highly different stabilities suggest a folding mechanism in which the intramembranous regions form a highly stable framework that may assist or even direct the folding of the extramembranous regions.

ACKNOWLEDGMENT

We thank Dr. W. Liu for performing the N-terminal sequence analysis, Scott D. Morrow for carrying out the large-scale cultivations, and J. F. Kolonay, Jr., for help with the polarographic measurements.

REFERENCES

Antholine, W. E., Kastrau, D. H., Steffens, G. C. M., Buse, G., Zumft, W. G., & Kroneck, P. M. H. (1992) *Eur. J. Biochem. 209*, 875–881.

Arrondo, J. L. R., Muga, A., Castresana, J., Bernabeu, C., & Goñi, F. (1989) *FEBS Lett. 252*, 118–120.

Arrondo, J. L. R., Muga, A., Castresana, J., & Goñi, F. (1993) *Prog. Biophys. Mol. Biol. 59*, 23–56.

Babcock, G. T., & Wikström, M. (1992) *Nature 356*, 301–309.

Brouillette, C. G., Muccio, D. D., & Finney, T. K. (1987) *Biochemistry 26*, 7431–7438.

Brouillette, C. G., McMichens, R. B., Stern, L. J., & Khorana, H. G. (1989) *Proteins 5*, 38–46.

Brunori, M., Antonini, G., Malatesta, F., Sarti, P., & Wilson, M. T. (1987) *Eur. J. Biochem. 169*, 1–8.

Capaldi, R. A. (1990) *Arch. Biochem. Biophys. 280*, 252–262.

Capaldi, R. A., Malatesta, F., & Darley-Usmar, V. (1983) *Biochim. Biophys. Acta 726*, 135–148.

Casey, R. P., Broger, C., & Azzi, A. (1981) *Biochim. Biophys. Acta 638*, 86–93.

Castresana, J., Muga, A., & Arrondo, J. L. R. (1988) *Biochem. Biophys. Res. Commun. 152*, 69–75.

Castresana, J., Fernandez-Ballester, G., Fernandez, A. M., Laynez, J. L., Arrondo, J. L. R., Ferragut, J. A., & Gonzalez-Ros, J. M. (1992) *FEBS Lett. 314*, 171–175.

Caughey, W. S., Dong, A., Sampath, V., Yoshikawa, S., & Zhao, X.-J. (1993) *J. Bioenerg. Biomembr. 25*, 81–91.

Chepuri, V., & Gennis, R. B. (1990) *J. Biol. Chem. 265*, 12978–12986.

Cowan, S. W. (1993) *Curr. Opin. Struct. Biol. 3*, 501–507.

Cramer, W. A., Engelman, D. M., von Heijne, G., & Rees, D. C. (1992) *FASEB J. 6*, 3397–3402.

Deatherage, J. F., Henderson, R., & Capaldi, R. A. (1982) *J. Mol. Biol. 158*, 501–514.

Degli Esposti, M., Crimi, M., & Venturoli, G. (1990) *Eur. J. Biochem. 190*, 207–219.

Engelman, D. M., Steiz, T. A., & Goldman, A. (1986) *Annu. Rev. Biophys. Biophys. Chem. 15*, 321–353.

Fernandez-Ballester, G., Castresana, J., Fernandez, A. M., Arrondo, J. L. R., Ferragut, J. A., & Gonzalez-Ros, J. M. (1994) *Biochemistry 33*, 4065–4071.

Freire, E., van Osdol, W. W., Mayorga, O. L., & Sanchez-Ruiz, J. M. (1990) *Annu. Rev. Biophys. Biophys. Chem. 19*, 159–188.

Frey, T. G., & Murray, J. M. (1994) *J. Mol. Biol. 237*, 275–297.

Haltia, T. (1992a) *Biochim. Biophys. Acta 1098*, 343–350.

Haltia, T. (1992b) *ICSU Short. Rep. 7*, 40.

Haltia, T., Finel, M., Harms, N., Nakari, T., Raitio, M., Wikström, M., & Saraste, M. (1989) *EMBO J. 8*, 3571–3579.

Haltia, T., Saraste, M., & Wikström, M. (1991) *EMBO J. 10*, 2015–2021.

Heibel, G. E., Hildebrandt, P., Ludwig, B., Steinrücke, P., Soulimane, T., & Buse, G. (1993) *Biochemistry 32*, 10866–10877.

Henderson, R., Baldwin, J. M., Ceska, T. A., Zemlin, F., Beckmann, E., & Downing, K. H. (1990) *J. Mol. Biol. 213*, 899–929.

Hill, B. C. (1991) *J. Biol. Chem. 266*, 2219–2226.

Hill, B. C., Cook, K., & Robinson, N. C. (1988) *Biochemistry 27*, 4741–4747.

Hosler, J. P., Ferguson-Miller, S., Calhoun, M., Thomas, J., Hill, J., Lemieux, L., Ma, J., Georgiou, C., Fetter, J., Shapleigh, J., Tecklenburg, M., Babcock, G. T., & Gennis, R. B. (1993) *J. Bioenerg. Biomembr. 25*, 121–136.

Kelly, M., Lappalainen, P., Talbo, G., Haltia, T., van der Oost, J., & Saraste, M. (1993) *J. Biol. Chem. 268*, 16781–16787.

Kroneck, P. M. H., Antholine, W. E., Riester, J., & Zumft, W. G. (1988) *FEBS Lett. 242*, 70–74.

Laemmli, U. K. (1970) *Nature 227*, 680–685.

Lappalainen, P., Aasa, R., Malmström, B. G., & Saraste, M. (1993) *J. Biol. Chem. 268*, 26416–26421.

Ludwig, B. (1986) *Methods Enzymol. 126*, 153–159.

Ludwig, B., & Schatz, G. (1980) *Proc. Natl. Acad. Sci. U.S.A. 77*, 196–200.

Malmström, B. G. (1993) *Acc. Chem. Res. 26*, 332–338.

Morin, P., Diggs, D., Montgomery, D., & Freire, E. (1990) *Biochemistry 29*, 781–788.

Muga, A., Arrondo, J. L. R., Bellon, T., Sancho, J., & Bernabeu, C. (1993) *Arch. Biochem. Biophys. 300*, 451–457.

Murphy, K. P., & Freire, E. (1992) *Adv. Protein Chem. 43*, 313–361.

Murphy, K. P., Bhakuni, V., Xie, D., & Freire, E. (1992) *J. Mol. Biol. 227*, 293–306.

Oikawa, K., Lieberman, D. M., & Reithmeier, R. A. F. (1985) *Biochemistry 24*, 2843–2848.

Picot, D., Loll, P. J., & Garavito, R. M. (1994) *Nature 367*, 243–249.

Popot, J.-L., & Engelman, D. M. (1990) *Biochemistry 29*, 4031–4037.

Power, S. D., Lochrie, M. A., & Poyton, R. O. (1986) *J. Biol. Chem. 261*, 9206–9209.

Prado, A., Muga, A., Castresana, J., Goñi, F. M., & Arrondo, J. L. R. (1990) *FEBS Lett. 269*, 324–327.

Privalov, P. L., & Gill, S. J. (1988) *Adv. Protein Chem. 39*, 191–234.

Raitio, M., Jalli, T., & Saraste, M. (1987) *EMBO J. 6*, 2825–2833.

Raitio, M., Pispa, J., Metso, T., & Saraste, M. (1990) *FEBS Lett. 261*, 431–435.

Rigell, C., & Freire, E. (1987) *Biochemistry 26*, 4366–4371.

Rigell, C., de Saussure, C., & Freire, E. (1985) *Biochemistry 24*, 5638–5646.

Saraste, M. (1990) *Q. Rev. Biophys. 23*, 331–366.

Schulz, G. E. (1993) *Curr. Opin. Cell Biol. 5*, 701–707.

Shnyrov, V. L., & Mateo, P. L. (1993) *FEBS Lett. 324*, 237–240.

Sone, N., Shimada, S., Ohmori, T., Souma, Y., Gonda, M., & Ishizuka, M. (1990) *FEBS Lett. 262*, 249–252.

Sone, N., Tano, H., & Ishizuka, M. (1993) *Biochim. Biophys. Acta 1183*, 130–138.

Spolar, R. S., Livingstone, J. R., & Record, M. T., Jr. (1992) *Biochemistry 31*, 3947–3955.

Steffens, G. C. M., Buse, G., Oppliger, W., & Ludwig, B. (1983) *Biochem. Biophys. Res. Commun. 116*, 335–340.

Steinrücke, P., Steffens, G. C. M., Panskus, G., Buse, G., & Ludwig, B. (1987) *Eur. J. Biochem. 167*, 431–439.

Steverding, D., Köhnke, D., Ludwig, B., & Kadenbach, B. (1993) *Eur. J. Biochem. 212*, 827–831.

Thomas, J. W., Puustinen, A., Alben, J. O., Gennis, R. B., & Wikström, M. (1993) *Biochemistry 32*, 10923–10928.

Valpuesta, J. M., Henderson, R., & Frey, T. G. (1990) *J. Mol. Biol. 214*, 237–251.

Wikström, M., Krab, K., & Saraste, M. (1981) *Cytochrome Oxidase—A Synthesis*, pp 44–48, Academic Press, London.

Yang, P. W., Mantsch, H. H., Arrondo, J. L. R., Saint-Girons, I., Guillou, Y., Cohen, G. N., & Barzu, O. (1987) *Biochemistry 26*, 2706–2711.

Yeates, T. (1993) in *Thermodynamics of Membrane Receptors and Channels* (Jackson, M. B., Ed.) pp 1–25, CRC Press, Boca Raton, FL.

Zhang, Y.-P., Lewis, R. N. A. H., Hodges, R. S., & McElhaney, R. N. (1992) *Biochemistry 31*, 11572–11578.

Zhang, Y.-Z., Lindorfer, M. A., & Capaldi, R. A. (1988) *Biochemistry 27*, 1389–1394.